Bioelectrochemistry 94 (2013) 87–93

Contents lists available at ScienceDirect

Bioelectrochemistry

journal homepage: www.elsevier.com/locate/bioelechem

The application of thionine–graphene nanocomposite in chiral sensing for Tryptophan enantiomers

Liju Guo, Qing Zhang, Yihan Huang, Qian Han, Yonghua Wang, Yingzi Fu *

Key Laboratory on Luminescence and Real-Time Analysis, Ministry of Education, School of Chemistry and Chemical Engineering, Southwest University, Chongqing 400715, China

ARTICLE INFO

Article history:
Received 4 June 2013
Received in revised form 28 August 2013
Accepted 1 September 2013
Available online 13 September 2013

Keywords:
Nano-bionic interface
Thionine–graphene nanocomposite
ds-DNA (Herring Sperm)
Chiral biosensor

ABSTRACT

The thionine–graphene (THi–GR, positively charged) nanocomposite was successfully synthesized as a good biocompatible matrix for ds-DNA which acted as a chiral selector to construct an electrochemical chiral biosensor for Tryptophan (Trp) enantiomers sensing with the assistance of Cu(II). The nano-bionic interface was constructed as follows: Firstly, the nanocomposite was dropped on the surface of glassy carbon electrode (GCE), and then ds-DNA (negatively charged) was immobilized onto the nanocomposite film via the opposite-charged adsorption techniques. This biofunctionalized nanocomposite was characterized with scanning electron microscopy (SEM), ultraviolet–visible (UV–vis) spectrometry and cyclic voltammetry (CV). The chiral biosensor was employed to study the recognition effect between ds-DNA and Trp enantiomers by CV. The results show that larger electrochemical response was obtained from L-Trp when Cu(II) was present, indicating this strategy could be employed to enantioselectively recognize Trp enantiomers. Under optimum conditions, the chiral biosensor exhibited a good linear response to Trp enantiomers in the range of the concentration of $[Cu(II)(Trp)_2]$ from 5.0×10^{-4} to 2.5 mM with a low limit of detection of 0.17 μM (S/N = 3). The binding constant was calculated to be 2.97×10^3 M^{-1} for $[Cu(II)(L\text{-}Trp)_2]$ and 2.50×10^2 M^{-1} for $[Cu(II)(D\text{-}Trp)_2]$.

1. Introduction

Graphene (GR), a single layer of sp^2 bonded carbon atoms in a honeycomb two-dimensional lattice, has attracted considerable attentions due to plenty of superior qualities, such as large specific surface, excellent electrical conductivity [1,2], high mechanical strength [3], prominent biocompatibility [4] and easy chemical modification by other groups and molecules [5]. Noticeable progress has been made in the utilization of graphene and graphene-based composites in recent years [6–9]. By virtue of the outstanding physical and chemical properties, graphene-based nanocomposites are increasingly attractive and have been designed towards applications in electrochemical biosensors [9–12]. For example, chitosan/graphene composite has been used to develop a sensitive electrochemical immunosensor for immunodetection of α-fetoprotein antigen [10], graphene-assisted signal amplification has been used in the sensitive detection of human IgG [13], a sensitive label-free electrochemical biosensor based on gold nanoparticles, polythionine, and graphene has been used to determine the sequence-specific target DNA [14]. Recently, a novel oligo(phenylene ethynylene)s/graphene nanocomposite has been synthesized to improve the electrocatalytic activity for dopamine determination [15], and a label-free electrochemical impedance genosensor based on 1-aminopyrene/graphene hybrids high has been fabricated for the detection of complementary oligonucleotide with high sensitivity and low detection limit [9]. Thionine (THi) is a redox dye including two amino groups, two aromatic rings and a heterocycle. Owing to its planar aromatic structure, THi is bound easily to the surface of GR via strong π–π stacking and synergistical noncovalent charge transfer [16]. The introduction of positively charged THi can improve the water solubility and prevent the aggregation of noncovalent functionalized GR [17]. Not only the GR, which owns excellent conductivity, can reinforce the electroactivity of THi, but also the THi can retain the intrinsic properties of GR [18]. Moreover, it is a favorable platform for the further biofunctionalization of the nanocomposite because of the existence of positively charged THi in nanocomposite. ds-DNA is a negatively charged biomolecule, which can be electrostatically attracted by THi and the bioactivity of ds-DNA will be retained to the largest extent on this nanocomposite, which is crucial for biosensing [19]. The thionine–graphene (THi–GR) nanocomposite combining the merits of GR with properties of THi has been used to fabricate a biosensor for detection of specific DNA sequence [2], but its biofunctionalization with ds-DNA to construct a nano-bionic interface for application in electrochemical chiral sensing has not been reported.

Enantiomers of a chiral molecule usually differ from each other in bioactivity and pharmacological behavior, of which one is useful for the body while the other is useless, even toxic [20]. Hence, the study of recognizing enantiomers is apparently significant. The interaction between ds-DNA and chiral molecules is an active subject in the area of life science, for instance, design of chemotherapeutic agents [21], function of DNA targeted drug, and mutation of genes [22]. The double stranded structure, usually right handed helical conformation, makes ds-DNA a natural chiral selector for chiral sensing of enantiomers. Additionally,

* Corresponding author. Tel.: +86 23 68252360; fax: +86 23 68253195.
E-mail address: fyzc@swu.edu.cn (Y. Fu).

1567-5394/$ – see front matter © 2013 Elsevier B.V. All rights reserved.
http://dx.doi.org/10.1016/j.bioelechem.2013.09.002

some transition metal ions (Cu(II), Ni(II), Zn(II), etc.) and their complexes are able to bind to ds-DNA [23], and specially the copper ions bind strongly to ds-DNA through the N7 of guanine [24,25]. The stereospecific interaction between the metal complexes of different conformations and ds-DNA can lead to different DNA-adduct profiles with different bioactivities, having been studied to design the new DNA targeted drug [26]. L-Tryptophan (L-Trp) is an essential amino acid of protein and a precursor of neurotransmitter serotonin [27]. The shortage of L-Trp in plasma may cause a number of chronic diseases [28]. To our pleasure, most amino acids including Trp can link with transition metal ions to form metal complexes with enantioselectivity very easily [29–32]. Owing to different interacting styles between ds-DNA and metal complexes of amino acids enantiomers, ds-DNA was chose as a selector for chiral sensing of Trp enantiomers in the presence of Cu(II).

In this work, a nano-bionic interface based on THi–GR nanocomposite and ds-DNA was designed as a chiral platform for Trp enantiomers sensing in the presence of Cu(II). The thionine–graphene (THi–GR) nanocomposite was first modified on the surface of glassy carbon electrode (GCE). Subsequently, ds-DNA was immobilized onto the nanocomposite film via electrostatic interaction between positively charged thionine (THi) and negatively charged ds-DNA, namely the opposite-charged adsorption techniques. This nanocomposite not only exhibited high electron transfer, but also could remain the bioactivity of ds-DNA to the largest extent. Moreover, instead of the traditional chiral recognition technique, the redox signal generated by the redox probe which was modified on the electrode could enhance electrochemical response of the chiral biosensor. Scanning electron microscope (SEM), ultraviolet–visible (UV–vis) spectrometry and cyclic voltammetry (CV) were employed to characterize the biofunctionalized THi–GR nanocomposite. This nano-bionic interface was employed to investigate the interaction between ds-DNA and Trp enantiomers by CV. Larger electrochemical response was obtained from [Cu(II)(L-Trp)$_2$]. The electrochemical signal difference for chiral recognition was obtained by monitoring the electrochemical response signal of Cu(II)/Cu(I) redox couple.

2. Experimental

2.1. Reagents and materials

L-Tryptophan (99%) and D-Tryptophan (99%) (L-Trp and D-Trp) were purchased from J&K chemical Co. (Beijing, China). Graphene oxide (GO) was obtained from Nanjing Xianfeng nano Co. (Nanjing, China). Herring Sperm double stranded DNA (ds-DNA, crude oligonucleotides, <50 bp), thionine (THi) and poly (ethylene imine) (PEI) were purchased from Sigma chemical Co. (St. Louis, MO, USA). $CuSO_4 \cdot 5H_2O$ was purchased from Chemical Reagent Co. (Chongqing, China). 0.1 M Phosphate buffer solution (PBS, pH 7.0) and 0.1 M HAc–NaAc buffer solution of various pH values were prepared. Other chemical reagents were analytical grade and used without further purification. Double distilled water was used in all experiments.

2.2. Apparatus

All electrochemical measurements were performed on a CHI 620D electrochemical workstation (Shanghai Chenhua Instruments, China), which was connected with a standard three-electrode system composed of a saturated calomel electrode (SCE) as the reference electrode, a platinum wire as the counter electrode, and a modified glassy carbon electrode (GCE) as the working electrode. The UV–vis absorption spectra were recorded by an UV-2450 spectrometer (Shimadzu, Japan). The scanning electron micrographs were taken with an S-4800 scanning electron microscope (SEM) at an acceleration voltage of 20 kV (Hitachi, Japan).

2.3. Preparation of THi–GR nanocomposite

GR was prepared by reducing GO according to literature reported previously [33]. In brief, reducing of GO was carried out via mixing 10 mL homogeneous dispersion of GO (1.0 mg/mL) with 1 mL PEI (3%) and refluxing for 3 h at 135 °C. Then the obtained black suspension was centrifuged and washed for several times to remove excessive PEI. The resulting GR was dispersed in water to be a stable suspension (1.0 mg/mL).

To prepare THi–GR nanocomposite, 5 mL suspension of GR (1.0 mg/mL) was mixed with 5 mL THi solution (1.2 mg/mL) and stirred at room temperature for 24 h. After removing excessive THi by centrifugation and washing with water, as-prepared THi–GR nanocomposite was dispersed in water (1.0 mg/mL).

2.4. Construction of the nano-bionic interface

Before construction, GCE ($\Phi = 4$ mm) was polished with 1.0, 0.3 and 0.05 μm alumina powders, respectively, rinsed thoroughly with double distilled water after each polishing, followed by successive ultrasonication in double distilled water and ethanol for 5 min. Subsequently, the GCE was subjected to cyclic scanning in sulfuric acid (0.5 M) ranging from −0.4 to 1.6 V at a scan rate of 0.1 V s^{-1} for 15 circles, and then dried at room temperature.

20 μL suspension of THi–GR nanocomposite was dropped onto the electrode surface and dried in the air. 8 μL ds-DNA (0.5 mg/mL) was prepared in 0.1 M PBS solution (pH 7.0), then it was dripped onto the surface to achieve the chiral biosensor modified with the nano-bionic interface (denoted as ds-DNA/THi–GR/GCE). After drying and washing, the chiral biosensor was ready for measurement. The stepwise procedure for assembly of the nano-bionic interface-based chiral biosensor is illustrated in Fig. 1.

3. Results and discussion

3.1. Characterization of the nano-bionic interface

3.1.1. SEM results

The morphologies of GR, THi–GR nanocomposite and ds-DNA–THi–GR nano-bionic interface were characterized with the SEM technique (Fig. 2A). As shown in Fig. 2A, the shape of GR is regularly flake like and slightly wrinkled (image a). The flake-like structure did not change significantly after the THi molecules were bound to the GR (image b). When ds-DNA was electrostatically adsorbed onto the surface of THi–GR nanocomposite, the morphology of ds-DNA–THi–GR nano-bionic interface still retained the basically flake-like structure and more irregular sheets aggregated together (image c).

3.1.2. UV–vis characterization

UV–vis spectrometry was performed to study the interaction among GR, THi and ds-DNA during the fabrication of the nano-bionic interface. UV–vis absorption spectra of GR, THi, THi–GR nanocomposite, ds-DNA, ds-DNA–THi–GR nano-bionic interface are illustrated in Fig. 2B. The spectrum of GR (curve a) exhibited an absorption maximum around 270 nm ascribed to the π-conjugation network of its structure. There were two characteristic absorption peaks in the spectrum of THi (curve b) that one was at 282 nm attributed to the π–π^* transitions of benzene rings and the other was around 600 nm corresponding to n–π^* transitions of C═N bond. When THi interacted with GR, the two characteristic absorption peaks can also be observed from the spectrum of THi–GR nanocomposite (curve c) with a bit blue shift and red shift, respectively, indicating the π–π interaction between THi and GR [2,16,34]. ds-DNA existing alone showed a characteristic absorption at 260 nm (curve d), which was in accordance with the report [35]. In the spectrum of ds-DNA–THi–GR nano-bionic interface (curve e), neither blue shift nor red shift appeared after ds-DNA interacted with the

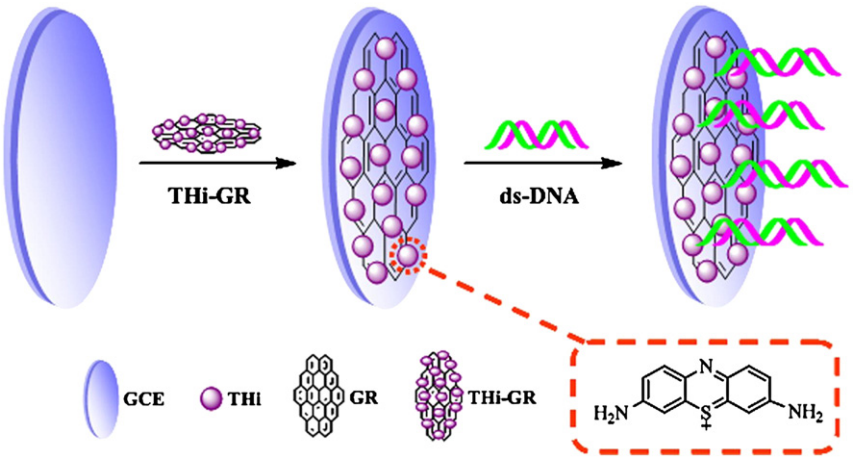

Fig. 1. Assembly of the nano-bionic interface-based chiral biosensor.

THi–GR nanocomposite, just a hypochromic effect, which demonstrated a typical electrostatic interaction between ds-DNA and the THi–GR nanocomposite [36]. This indicates ds-DNA has been successfully assembled on the surface of the nanocomposite via THi as mediator and ds-DNA still maintained its native structure [37]. All the results suggest that the nano-bionic interface has been successfully constructed.

3.1.3. Electrochemical characterization of different interfaces

CV was used to study the electrochemical behaviors of different interfaces modified electrodes in 0.1 M HAc–NaAc buffer solution (pH 5.5) at the scan rate of 0.1 V s^{-1}. As shown in Fig. 3, CV of each modified step is recorded from −0.6 to 0.3 V. There were no evident peaks on bare GCE (curve a) and GR modified GCE (denoted as GR/GCE, curve b). In contrast with GR/GCE, a couple of well-defined redox peaks with the high peak currents was obtained after the THi–GR nanocomposite was immobilized onto the surface of GCE (denoted as THi–GR/GCE, curve c). It was attributed to the excellent electronic transport property, high stability of GR and the good electroactivity of THi. Afterwards, ds-DNA was bound to the surface of THi–GR/GCE through noncovalent electrostatic interaction between ds-DNA and THi–GR nanocomposite [38,39], leading to some obvious decrease of the peak currents (denoted as ds-DNA/THi–GR/GCE, curve d). This resulted from that ds-DNA formed an electron-transfer blocking layer inhibiting the electron transporting but the good electronic transport property of THi–GR nanocomposite improved this situation. Compared with the conventional means by using $[Fe(CN)_6]^{4-/3-}$ in the electrolyte as the redox probe, THi in the nano-bionic interface modified on the electrode undoubtedly acted as a perfect redox mediator and a good linker to the chiral selector. Moreover, the THi–GR nanocomposite could provide a well biocompatible microenvironment for ds-DNA to stabilize its biological activity. Due to this interface as the chiral sensing platform, the electrochemical chiral biosensor exhibited good response for the chiral sensing of Trp enantiomers. The effect of the scan rate on the nano-bionic interface modified electrode was also investigated. The experimental result shows that both anodic and cathodic current presented good linear dependence of square root of the scan rate, which indicates that the redox reaction of THi in the nano-bionic interface was a diffusion controlled process [40]. The redox reaction of the electroactive THi can be described by the following equation in Scheme 1:

3.2. ds-DNA–THi–GR nano-bionic interface for Trp enantiomer sensing

CV measurements were carried out in 0.1 M HAc–NaAc buffer solution (pH 5.5) to record the electrochemical responses before and after the ds-DNA–THi–GR nano-bionic interface-based chiral biosensor interacted with Trp enantiomers. The peak currents augmented after the ds-DNA/THi–GR/GCE (curve a and curve b) was incubated in 5.0 mM L-Trp or D-Trp in the presence of 2.5 mM Cu(II) for 20 min (Fig. 4A). It was assumed that the attack of Cu complexes to ds-DNA caused the augmentation of peak currents and the electrochemical signal for the stereoselective interaction between ds-DNA and $[Cu(II)(L\text{-}Trp)_2]$ or $[Cu(II)(D\text{-}Trp)_2]$ was detected from the signal of Cu(II)/Cu(I) redox couple [41]. The redox reaction can be expressed as follows:

$$\left[Cu(II)(D/L\text{-}Trp)_2\right] + THi^+ + H^+ + 3e^- \rightleftharpoons \left[Cu(I)(D/L\text{-}Trp)_2\right] + LTHi. \quad (1)$$

From the CVs in Fig. 4A, it can be seen that a larger increase of anodic peak current was attained from $[Cu(II)(L\text{-}Trp)_2]$ (curve c) than that from $[Cu(II)(D\text{-}Trp)_2]$ (curve d), and the average difference between ΔI_{pL} ($\Delta I_{pL} = I_{pL} - I_p$) and ΔI_{pD} ($\Delta I_{pD} = I_{pD} - I_p$) was 20.5 μA (RSD = 3.9%, n = 5). What was gained implied the amount of $[Cu(II)(L\text{-}Trp)_2]$ adsorbed on the ds-DNA/THi–GR/GCE was more than that of $[Cu(II)(D\text{-}Trp)_2]$. It further certified that $[Cu(II)(L\text{-}Trp)_2]$ bound more easily to ds-DNA than $[Cu(II)(D\text{-}Trp)_2]$ did. The higher stereospecific selection of ds-DNA to $[Cu(II)(L\text{-}Trp)_2]$ when forming ds-DNA–$[Cu(II)(Trp)_2]$ complex was mainly achieved through electrostatic interaction via the phosphate skeleton of ds-DNA [26].

To explore the importance on Cu(II), the situation without Cu(II) was investigated. As shown in Fig. 4B, ds-DNA/THi–GR/GCE (curve a and curve b) presented a couple of well-defined redox peaks. After ds-DNA/THi–GR/GCE was incubated in 5.0 mM L-Trp or D-Trp without Cu(II), the peak currents descended with the variation of time and reached to constance after some minutes indicating the existence of the interaction between ds-DNA and Trp, but there was almost no difference between the peak currents of ds-DNA/THi–GR/GCE incubated in L-Trp (curve c) and D-Trp (curve d) in the absence of Cu(II) after 20 min or even longer time. All the results demonstrated the signal for chiral recognition was ascribable to the Cu(II)/Cu(I) redox couple and Cu(II) played an important role in the enantioselective discrimination.

3.3. Optimization of experimental conditions

3.3.1. Effect of pH

The pH of the working buffer solution has a great effect on the electrochemical behavior of the designed chiral biosensor, which will affect the chiral recognition. The influence of pH on the peak current response of the chiral biosensor was tested in 0.1 M HAc–NaAc buffer solution from pH 4.0 to pH 7.0 (Fig. 5A). There came the largest anodic peak current at pH 5.5 (RSD = 1.3%, n = 5), and a couple of well-defined redox

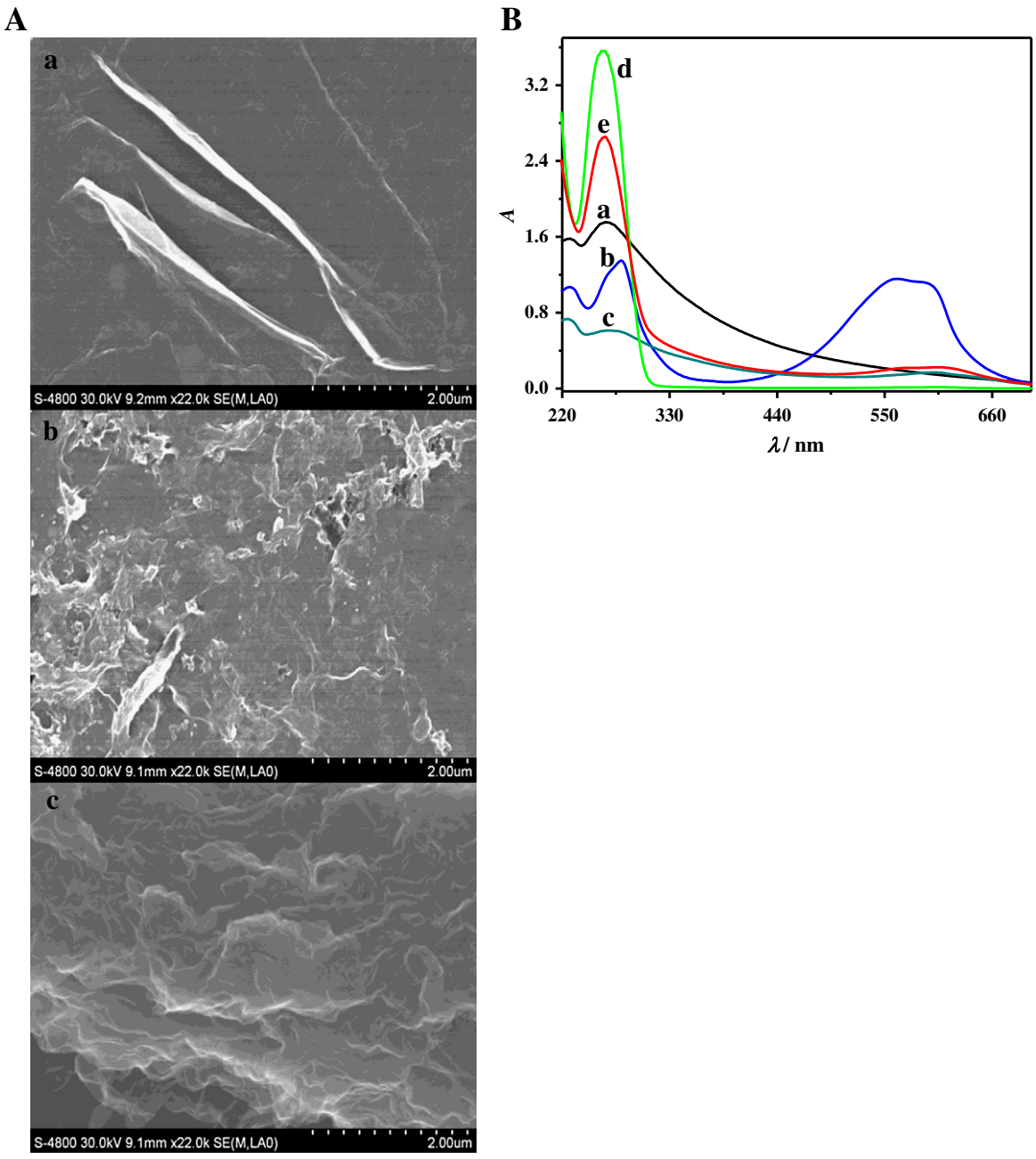

Fig. 2. (A) SEM images. (a) GR, (b) THi–GR nanocomposite and (c) ds-DNA–THi–GR nano-bionic interface. (B) UV–vis absorption spectra. (a) GR, (b) THi, (c) THi–GR nanocomposite, (d) ds-DNA and (e) ds-DNA–THi–GR nano-bionic interface.

peaks was presented at the pH value. Therefore, pH 5.5 HAc–NaAc buffer solution was used as the working buffer solution throughout the experiments.

3.3.2. The influence of incubation time

It is important to investigate incubation time of ds-DNA/THi–GR/GCE in [Cu(II)(Trp)$_2$]. Fig. 5B describes the influence of incubation time from 0 to 35 min, demonstrating the time dependence of the increase of anodic peak current when the chiral biosensor interacted with [Cu(II)(L-Trp)$_2$] or [Cu(II)(D-Trp)$_2$]. It shows that the current response from [Cu(II)(L-Trp)$_2$] increased fast and sharply, and even was always larger than that from [Cu(II)(D-Trp)$_2$], owing to the faster attack of [Cu(II)(L-Trp)$_2$] to ds-DNA and the more [Cu(II)(L-Trp)$_2$] adsorbed onto the modified electrode. When the obvious and maximum electrochemical signal difference emerged at 20 min (RSD = 1.0%, n = 5), therefore, 20 min was selected as the optimized time for the chiral recognition.

3.4. Performance of the chiral biosensor

The anodic peak current responses after the chiral biosensor interacted with L-Trp and D-Trp solution containing Cu(II) at a series of concentrations are illustrated in Fig. 6. As shown, the anodic peak current change (ΔI_{pL} or ΔI_{pD}) increased with the increasing concentration of [Cu(II)(L-Trp)$_2$] or [Cu(II)(D-Trp)$_2$]. Under optimized conditions, the peak current change of ds-DNA/THi–GR/GCE incubated in [Cu(II)(L-Trp)$_2$] (curve a) was always larger than [Cu(II)(D-Trp)$_2$] (curve b) at all concentrations, further certifying that ds-DNA had a higher affinity

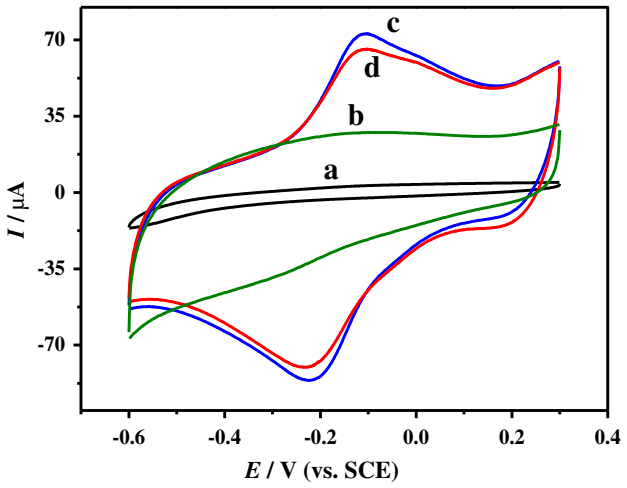

Fig. 3. CVs of different interfaces in 0.1 M HAc–NaAc buffer solution (pH 5.5). (a) bare GCE, (b) GR/GCE, (c) THi–GR/GCE and (d) ds-DNA/THi–GR/GCE.

to [Cu(II)(L-Trp)$_2$] than [Cu(II)(D-Trp)$_2$]. The chiral biosensor exhibited a good linear response to Trp enantiomers in the range of the concentration of [Cu(II)(Trp)$_2$] from 5.0×10^{-4} to 2.5 mM with a low limit of detection of 0.17 μM (S/N = 3). The linear regression equations are y_L (μA) = 27.34 × (mM) + 7.433(±0.0005) with R_L = 0.9981 and y_D (μA) = 20.75 × (mM) + 5.867(±0.0005) with R_D = 0.9927, respectively. In order to estimate the effect of substrate for chiral recognition, calibration plots without the ds-DNA at the same conditions are shown in Fig. 6. As shown, the peak current change was not apparent, and there was almost no difference between the ΔI_{pL} and ΔI_{pD} after THi–GR/GCE was incubated in [Cu(II)(L-Trp)$_2$] (curve c) and [Cu(II)(D-Trp)$_2$] (curve d), respectively. All of above results demonstrate the proposed electrochemical chiral biosensor could be used for the chiral discrimination of Trp.

3.5. Determination of the binding constant

To quantify the difference of DNA binding between [Cu(II)(L-Trp)$_2$] and [Cu(II)(D-Trp)$_2$] in this recognition strategy, the binding constant was calculated. The value of the binding constant between DNA and [Cu(II)(L-Trp)$_2$] or [Cu(II)(D-Trp)$_2$], K, and the binding number, m, can be determined by the Eq. (1) [42,43]:

$$\log(\Delta I/(\Delta I_{max}-\Delta I)) = \log K + m\log([\mathrm{Cu(II)(Trp)_2}]/\mathrm{M}) \quad (2)$$

where ΔI is the peak current change after the ds-DNA/THi–GR/GCE interacted with [Cu(II)(L-Trp)$_2$] or [Cu(II)(D-Trp)$_2$], ΔI_{max} is the maximum peak current change, and [Cu(II)(Trp)$_2$] is the molar concentration of [Cu(II)(Trp)$_2$].

When the quantity of ds-DNA was kept constant and the concentration of [Cu(II)(Trp)$_2$] was changed from 5.0×10^{-7} to 2.5×10^{-3} M, the plot of correlation between $\log(\Delta I/(\Delta I_{max} - \Delta I))$ and log([Cu(II)(Trp)$_2$]) was obtained with the mean value of ΔI (n = 5) and is presented in Fig. 7. As shown, the value of $\log(\Delta I/(\Delta I_{max} - \Delta I))$ is linear with both log([Cu(II)(L-Trp)$_2$]) (curve a) and log([Cu(II)(D-Trp)$_2$]) (curve b). The linear equation are y_L = 0.9124 × (M) + 3.473(±0.0005) (R_L = 0.9959) and y_D = 0.6022 × (M) + 2.398(±0.0005) (R_D = 0.9968), respectively. Based on the intercept of the linear plot, K_L was calculated to be 2.97×10^3 M^{-1} and K_D was 2.50×10^2 M^{-1}. According to the slope, both m = 1 were obtained. Herein, [Cu(II)(Trp)$_2$] bound to ds-DNA formed 1:1 complex, and K_L was larger than K_D, which further suggested that the binding of ds-DNA to [Cu(II)(L-Trp)$_2$] was much stronger than to [Cu(II)(D-Trp)$_2$].

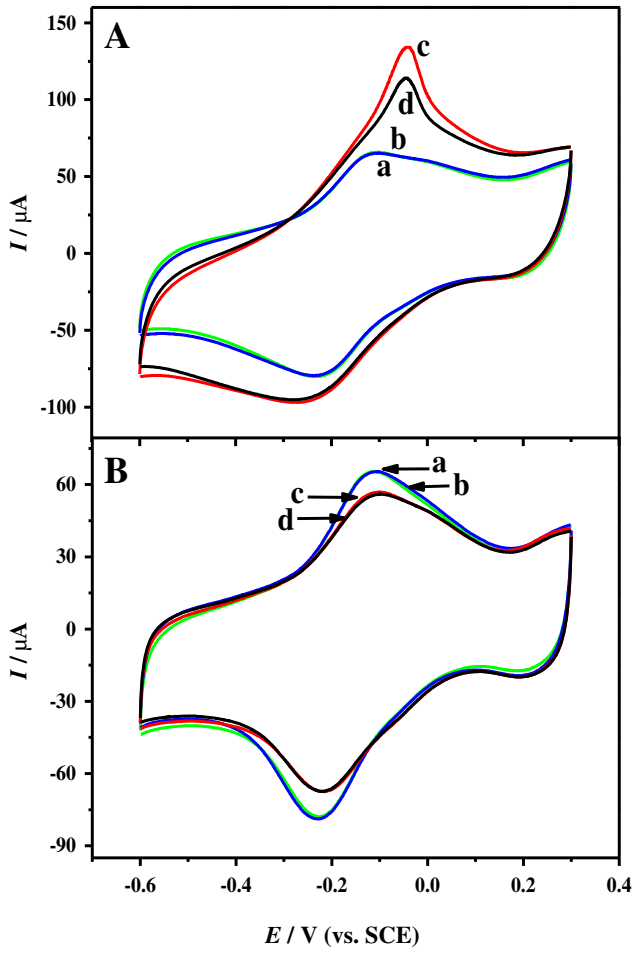

Fig. 4. (A) CVs of the interaction of the nano-bionic interface with 5.0 mM Trp enantiomers in the presence of 2.5 mM Cu(II). (a and b) ds-DNA/THi–GR/GCE, (c) after incubated in [Cu(II)(L-Trp)$_2$] and (d) [Cu(II)(D-Trp)$_2$] for 20 min, respectively. (B) CVs of the interaction of the nano-bionic interface with 5.0 mM Trp enantiomers in the absence of Cu(II). (a and b) ds-DNA/THi–GR/GCE, (c) after incubated in L-Trp and (d) D-Trp for 20 min, respectively.

4. Conclusions

In summary, a chiral biosensor for Trp enantiomers sensing was constructed. The THi–GR nanocomposite combining the good electronic transport and biocompatible properties of GR with the excellent electroactivity of THi was employed to immobilize ds-DNA. In the presence of Cu(II), larger response was obtained from L-Trp and the chiral biosensor exhibited a good linear response to Trp enantiomers with a low limit of detection. The easy preparation and excellent performance of

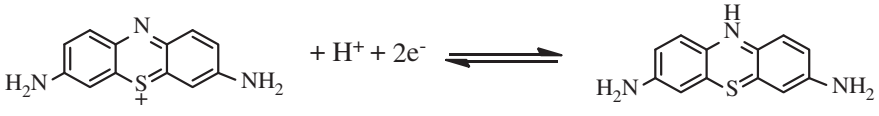

Thionine(THi) Leucothionine(LTHi)

Scheme 1. Schematic representation of the redox reaction of thionine.

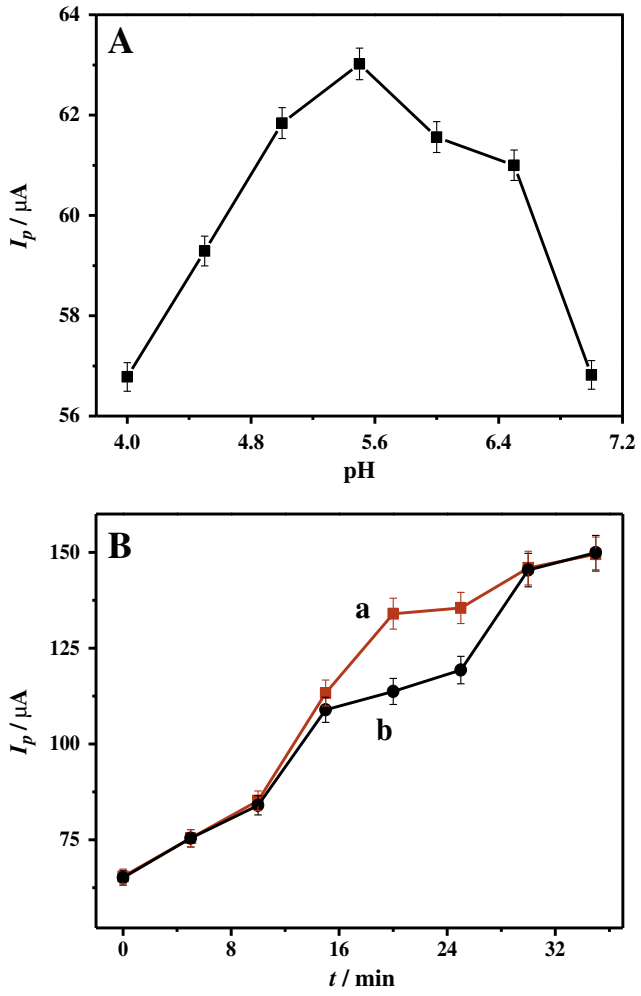

Fig. 5. (A) The effect of pH on the current response of the nano-bionic interface in 0.1 M HAc–NaAc buffer solution. (B) The influence of incubation time on the current response of the nano-bionic interface: (a) incubated in [Cu(II)(L-Trp)$_2$] and (b) [Cu(II)(D-Trp)$_2$] solution.

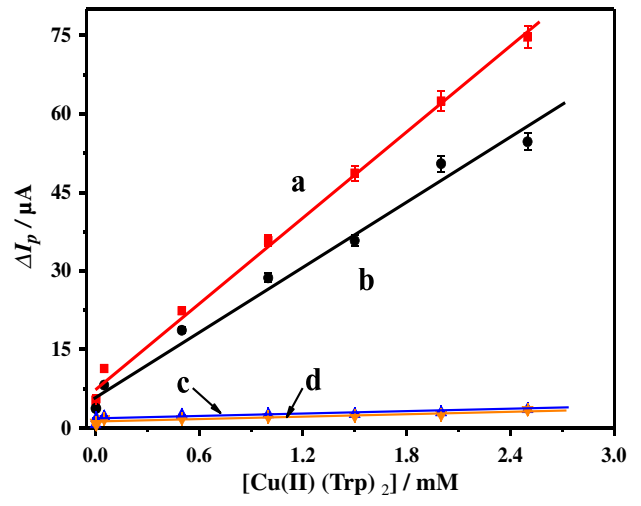

Fig. 6. Calibration plots of the peak current change at different concentrations: 5.0×10^{-4}, 5.0×10^{-3}, 5.0×10^{-2}, 5.0×10^{-1}, 1.0, 1.5, 2.0, 2.5 mM. (a) and (b) ds-DNA/THi–GR/GCE after incubated in [Cu(II)(L-Trp)$_2$] and [Cu(II)(D-Trp)$_2$], respectively, linear regression equations: y_L (μA) = 27.34 × (mM) + 7.433(±0.0005) (R_L = 0.9981) and y_D (μA) = 20.75 × (mM) + 5.867(±0.0005) (R_D = 0.9927), (c) and (d) THi–GR/GCE after incubated in [Cu(II)(L-Trp)$_2$] and [Cu(II)(D-Trp)$_2$], respectively.

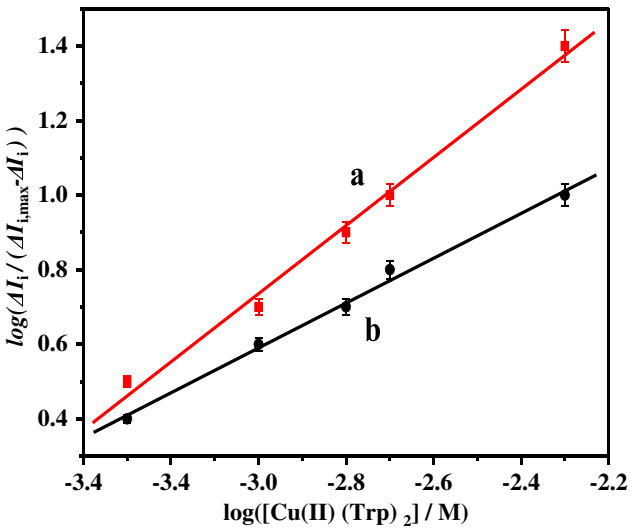

Fig. 7. The plot of dependence of $\log(\Delta I/(\Delta I_{max} - \Delta I))$ on log[Cu(II)(Trp)$_2$]. (a) [Cu(II)(L-Trp)$_2$] and (b) [Cu(II)(D-Trp)$_2$], linear regression equations: $y_L = 0.9124 \times (M) + 3.473(\pm 0.0005)$ ($R_L = 0.9959$) and $y_D = 0.6022 \times (M) + 2.398(\pm 0.0005)$ ($R_D = 0.9968$).

the chiral biosensor suggest that the development and application of the biocompatible and redox-active nanomaterials is an attractive subject in enantioselective recognition. Meanwhile, this work is very expected to provide a novel model for chiral sensing of other chiral drugs and may provide useful information for the study of new DNA targeted drugs.

Acknowledgments

This work was supported by the National Natural Science Foundation of China (Nos. 20972128 and 21272188).

References

[1] Y. Bo, H.Y. Yang, Y. Hu, T.M. Yao, S.S. Huang, A novel electrochemical DNA biosensor based on graphene and polyaniline, Electrochim. Acta 56 (2011) 2676–2681.
[2] L.M. Zhu, L.Q. Luo, Z.X. Wang, DNA electrochemical biosensor based on thionine–graphene nanocomposite, Biosens. Bioelectron. 35 (2012) 507–511.
[3] K.S. Novoselov, A.K. Geim, S.V. Morozov, D. Jiang, Y. Zhang, S.V. Dubonos, I.V. Grigorieva, A.A. Firsov, Electric field effect in atomically thin carbon films, Science 306 (2004) 666–669.
[4] H.Q. Chen, M.B. Müller, K.J. Gilmore, G.G. Wallace, D. Li, Mechanically strong, electrically conductive, and biocompatible graphene paper, Adv. Mater. 20 (2008) 3557–3561.
[5] Y.L. Cui, B. Zhang, B.Q. Liu, H.F. Chen, G.N. Chen, D.P. Tang, Sensitive detection of hydrogen peroxide in foodstuff using an organic–inorganic hybrid multilayer-functionalized graphene biosensing platform, Microchim. Acta 174 (2011) 137–144.
[6] K. Kim, H.J. Park, B.-C. Woo, K.J. Kim, G.T. Kim, W.S. Yun, Electric property evolution of structurally defected multilayer grapheme, Nano Lett. 8 (2008) 3092–3096.
[7] M. Zhou, Y.M. Zhai, S.J. Dong, Electrochemical sensing and biosensing platform based on chemically reduced graphene oxide, Anal. Chem. 81 (2009) 5603–5613.
[8] X.Z. Shi, H. Gong, Y.J. Li, C. Wang, L. Cheng, Z. Liu, Graphene-based magnetic plasmonic nanocomposite for dual bioimaging and photothermal therapy, Biomaterials 34 (2013) 4786–4793.
[9] L.Q. Luo, Z. Zhang, Y.P. Ding, D.M. Deng, X.L. Zhu, Z.X. Wang, Label-free electrochemical impedance genosensor based on 1-aminopyrene/graphene hybrids, Nanoscale 5 (2013) 5833–5840.
[10] D. Du, Z.X. Zou, Y. Shin, J. Wang, H. Wu, M.H. Engelhard, J. Liu, I.A. Aksay, Y.H. Lin, Sensitive immunosensor for cancer biomarker based on dual signal amplification strategy of graphene sheets and multienzyme functionalized carbon nanospheres, Anal. Chem. 82 (2010) 2989–2995.
[11] C.S. Shan, H.F. Yang, D.X. Han, Q.X. Zhang, A. Ivaska, L. Niu, Water-soluble graphene covalently functionalized by biocompatible poly-L-lysine, Langmuir 25 (2009) 12030–12033.
[12] K.F. Zhou, Y.H. Zhu, X.L. Yang, J. Luo, C.Z. Li, S.R. Luan, A novel hydrogen peroxide biosensor based on Au–graphene–HRP–chitosan biocomposites, Electrochim. Acta 55 (2010) 3055–3060.
[13] K.P. Liu, J.J. Zhang, C.M. Wang, J.J. Zhu, Graphene-assisted dual amplification strategy for the fabrication of sensitive amperometric immunosensor, Biosens. Bioelectron. 26 (2011) 3627–3632.
[14] Y.Z. Zhang, L. Huang, Label-free electrochemical DNA biosensor based on a glassy carbon electrode modified with gold nanoparticles, polythionine, and graphene, Microchim. Acta 176 (2012) 463–470.

[15] J.H. Deng, M.L. Liu, F.B. Lin, Y.Y. Zhang, Y. Liu, S.Z. Yao, Self-assembled oligo(phenylene ethynylene)s/grapheme nanocomposite with improved electrochemical performances for dopamine determination, Anal. Chim. Acta 767 (2013) 59–65.
[16] C. Chen, W.T. Zhai, D.D. Lu, H.B. Zhang, W.G. Zheng, A facile method to prepare stable noncovalent functionalized graphene solution with thionine, Mater. Res. Bull. 46 (2011) 583–587.
[17] Y. Zhuo, R. Yuan, Y.Q. Chai, Y. Zhang, X.L. Li, N. Wang, Q. Zhu, Amperometric enzyme immunosensors based on layer-by-layer assembly of gold nanoparticles and thionine on Nafion modified electrode surface for α-1-fetoprotein determinations, Sensors Actuators B Chem. 114 (2006) 631–639.
[18] A. Ghosh, K.V. Rao, S.J. George, C.N.R. Rao, Noncovalent functionalization, exfoliation, and solubilization of graphene in water by employing a fluorescent coronene carboxylate, Chem. Eur. J. 16 (2010) 2700–2704.
[19] T. Kuila, S. Bose, P. Khanra, A.K. Mishra, N.H. Kimc, J.H. Lee, Recent advances in graphene-based biosensors, Biosens. Bioelectron. 26 (2011) 4637–4648.
[20] J.A. Switzer, H.M. Kothari, Ph. Poizot, S. Nakanishi, E.W. Bohannan, Enantiospecific electrodeposition of a chiral catalyst, Nature 425 (2003) 490–493.
[21] G. Facchin, E. Kremer, D.A. Barrio, S.B. Etcheverry, A.J. Costa-Filho, M.H. Torre, Interaction of Cu-dipeptide complexes with Calf Thymus DNA and antiproliferative activity of [Cu(ala-phe)] in osteosarcoma-derived cells, Polyhedron 28 (2009) 2329–2334.
[22] T.T. Gu, Y. Hasebeb, Novel amperometric assay for drug–DNA interaction based on an inhibitory effect on an electrocatalytic activity of DNA–Cu(II) complex, Biosens. Bioelectron. 33 (2012) 222–227.
[23] H. Richard, J.P. Schereiber, M. Daune, Interactions of metallic ions with DNA. V. DNA renaturation mechanism in the presence of Cu^{2+}, Biopolymers 12 (1973) 1–10.
[24] Y.G. Gao, M. Sriam, A.H.J. Wang, Crystallographic studies of metal ion–DNA interactions: different binding modes of cobalt(II), copper(II) and barium(II) to N7 of guanines in Z-DNA and a drug–DNA complex, Nucleic Acid Res. 21 (1993) 4093–4191.
[25] B.H. Geierstanger, T.F. Kagawa, S.L. Chen, G.J. Quigley, P.S. Ho, Base-specific binding of Copper(II) to Z-DNA. The 1.3-Å single crystal structure of d(m6CGUAm6CG) in the presence of CuCl2, J. Biol. Chem. 266 (1991) 20185–20191.
[26] F. Arjmand, M. Muddassir, R.H. Khan, Chiral preference of L-tryptophan derived metal-based antitumor agent of late 3d-metal ions (Co(II), Cu(II) and Zn(II)) in comparison to D- and DL-tryptophan analogues: their in vitro reactivity towards CT DNA, 5′-GMP and 5′-TMP, Eur. J. Med. Chem. 45 (2010) 3549–3557.
[27] S.Z. Kang, H. Chen, X.Q. Li, J. Mu, Preparation of l-alanine ethyl ester modified multiwalled carbon nanotubes and their chiral discrimination between D- and L-tryptophan, Diam. Relat. Mater. 19 (2010) 1221–1224.
[28] J.B. Raoof, R. Ojani, H. Karimi-Maleh, Carbon paste electrode incorporating 1-[4-(ferrocenyl ethynyl) phenyl]-1-ethanone for electrocatalytic and voltammetric determination of tryptophan, Electroanalysis 20 (2008) 1259–1262.
[29] W.R. Yang, J.J. Gooding, D.B. Hibbert, Characterisation of gold electrodes modified with self-assembled monolayers of l-cysteine for the adsorptive stripping analysis of copper, J. Electroanal. Chem. 516 (2001) 10–16.
[30] T. Bauer, J. Gajewiak, α-Hydroxy carboxylic acids as ligands for enantioselective diethylzinc additions to aromatic and aliphatic aldehydes, Tetrahedron 60 (2004) 9163–9170.
[31] J.J. Gooding, D.B. Hibbert, W. Yang, Electrochemical metal ion sensors. Exploiting amino acids and peptides as recognition elements, Sensors 1 (2001) 75–90.
[32] M. Matsunaga, T. Nakanishi, T. Asahi, T. Osaka, Highly enantioselective discrimination of amino acids using copper deposition on a gold electrode modified with homocysteine monolayer, Electrochem. Commun. 9 (2007) 725–728.
[33] L.Y. Cao, Y.L. Liu, B.H. Zhang, L.H. Lu, In situ controllable growth of prussian blue nanocubes on reduced graphene oxide: facile synthesis and their application as enhanced nanoelectrocatalyst for H_2O_2 reduction, ACS Appl. Mater. Interfaces 2 (2010) 2339–2346.
[34] Q. Wei, K.X. Mao, D. Wu, Y.X. Dai, J. Yang, B. Du, M.H. Yang, H. Li, A novel label-free electrochemical immunosensor based on graphene and thionine nanocomposite, Sensors Actuators B Chem. 149 (2010) 314–318.
[35] S.R. Bhattarai, S. Aryal, K.C. Remant Bahadur, N. Bhattarai, P.H. Hwang, H.K. Yi, H.Y. Kim, Carbon nanotube-hydroxyapatite nanocomposite for DNA complexation, Mater. Sci. Eng. C 28 (2008) 64–69.
[36] R.S. Kumar, S. Arunachalam, Synthesis, characterization and DNA binding studies of a polymer-cobalt(III) complex containing the 2,2′-bipyridyl ligand, Polyhedron 25 (2006) 3113–3117.
[37] M.J. Gong, T. Han, C.X. Cai, T.H. Lu, J.Y. Du, Fabrication and characterization of DNA–thionine–carbon nanotube nanocomposites, J. Electroanal. Chem. 623 (2008) 8–14.
[38] C.F. Ou, R. Yuan, Y.Q. Chai, M.Y. Tang, R. Chai, X.L. He, A novel amperometric immunosensor based on layer-by-layer assembly of gold nanoparticles-multi-walled carbon nanotubes–thionine multilayer films on polyelectrolyte surface, Anal. Chim. Acta 603 (2007) 205–213.
[39] Q.W. Li, J. Zhang, H. Yan, M.S. He, Z.F. Liu, Thionine-mediated chemistry of carbon nanotubes, Carbon 42 (2004) 287–291.
[40] D.P. Tang, R. Yuan, Y.Q. Chai, Electron-transfer mediator microbiosensor fabrication based on immobilizing HRP-labeled Au colloids on gold electrode surface by 11-mercaptoundecanoic acid monolayer, Electroanalysis 18 (2006) 259–266.
[41] T.T. Gu, Y. Hasebeb, DNA–Cu(II) poly(amine) complex membrane as novel catalytic layer for highly sensitive amperometric determination of hydrogen peroxide, Biosens. Bioelectron. 21 (2006) 2121–2128.
[42] F. Qu, N.Q. Li, Y.Y. Jiang, Electrochemical studies of NiTMpyP and interaction with DNA, Talanta 45 (1998) 787–793.
[43] Y.H. Wu, X.B. Ji, S.S. Hu, Studies on electrochemical oxidation of azithromycin and its interaction with bovine serum albumin, Bioelectrochemistry 64 (2004) 91–97.

Liju Guo is a MS candidate in the College of Chemistry and Chemical Engineering of Southwest University, China. Her main interests are the development and application of nanomaterials in electrochemical biosensors and chiral recognition.

Qing Zhang is a MS candidate in the College of Chemistry and Chemical Engineering of Southwest University, China and is interested in the development of electrochemical chiral sensors.

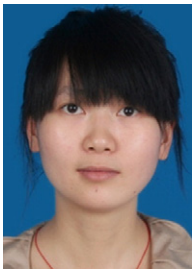

Yihan Huang is a MS candidate in the College of Chemistry and Chemical Engineering of Southwest University, China. She goes in for the study of chiral recognition mechanism.

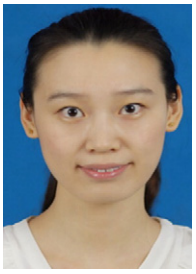

Qian Han is a MS candidate in the College of Chemistry and Chemical Engineering of Southwest University, China. She is interested in the development of electrochemical chiral sensors and methods for chiral recognition.

Yonghua Wang is a MS candidate in the College of Chemistry and Chemical Engineering of Southwest University, China. She has much interest in the chiral analysis.

Yingzi Fu is a professor in the College of Chemistry and Chemical Engineering of Southwest University, China. She received PhD degree in analytical chemistry from this university in 2006. The main research interests of Prof. Fu are nanomaterials, biosensors as well as the development and application of electrochemical chiral sensors.